

Dielectric relaxation in the smectic- A^* and smectic- C^* phases of a ferroelectric liquid crystal

A. M. Biradar,* S. Wróbel,[†] and W. Haase

Institut für Physikalische Chemie, Technische Hochschule, Petersenstrasse 20, D-6100 Darmstadt, Federal Republic of Germany

(Received 16 August 1988)

The results of a study of the dielectric properties of a room-temperature ferroelectric liquid crystal in the frequency range from 5 Hz to 13 MHz are presented here. Measurements of complex electric permittivity versus temperature have been taken on aligned samples of different thicknesses with the electric measuring field being parallel or perpendicular to the layer planes. In homogeneously aligned samples two dielectric relaxation regions have been observed in the smectic- C^* phase, one known as the Goldstone mode and the other showing up in the vicinity of the smectic- C^* -smectic- A^* transition called the soft mode. In homeotropically aligned samples the low-frequency molecular relaxation was observed in both smectic phases. Temperature dependences of both dielectric increments and relaxation times suggest that the system studied exhibits a ferroelectric phase transition of the first-order type.

I. INTRODUCTION

In 1975 the existence of ferroelectric liquid crystals was reported for the first time by Meyer *et al.*¹ Since then, considerable experimental and theoretical progress has been made in understanding the behavior of the smectic- C^* phase, which shows ferroelectric properties. The temperature dependence of the tilt, the spontaneous polarization, and the pitch of the helix can be calculated from experimental data and are in good agreement with the theory. Comparatively few studies have been reported regarding the dielectric properties of the ferroelectric liquid crystals, which hold a special interest in the field of liquid crystals, as one can observe the influence of the helicoidal texture that is characteristic of these materials.

The dielectric properties of the smectic- A^* -smectic- C^* (Sm- A^* -Sm- C^*) transition of ferroelectric liquid crystals have been the subject of many experimental and theoretical investigations. Most studies are concerned with the well-known compound DOBAMBC (*p*-decyloxybenzylidene-*p*-amino-2-methylbutyl cinamate). In a few papers²⁻⁴ the dielectric relaxation studies in this material have been reported and the two important relaxation modes, i.e., the Goldstone and soft mode, have been found theoretically and experimentally. It was shown that the Goldstone mode appears in the Sm- C^* phase because of the phase fluctuations in the azimuthal orientation of the director. The soft mode appears only at the transition temperature and a few degrees above the transition temperature in the Sm- A^* phase due to the fluctuations in the amplitude of the tilt angle. But recently, Levstik *et al.*⁵ have shown theoretically and experimentally in a ferroelectric liquid-crystal mixture that the soft mode can appear in both the phases very close to the transition temperature Sm- C^* -Sm- A^* .

In this paper we present the results of experiments in which the dielectric spectra of a room-temperature ferroelectric liquid crystal have been studied as a function of

frequency and temperature. For both fundamental research and practical applications it is a great advantage if a compound possesses the Sm- C^* phase at room temperature. The room-temperature ferroelectric liquid-crystal mixture which consists of a few compounds⁶ was available from E. Merck, Darmstadt (code name ZLI-3654). Two basic compounds of the ZLI-3654 mixture responsible for its dielectric properties are shown in Table I together with the phase diagram of the mixture.

II. EXPERIMENT

Complex electric permittivity was measured in cells of the sandwich type. Gold-coated glass plates were used for electrodes. The measurements were performed in two configurations as shown in Fig. 1. In the perpendicular configuration (homogeneous) the smectic layer planes are perpendicular to the glass plates, and in the parallel configuration (homeotropic) they are parallel to the glass plates. This means that in the former case the electric measuring field is parallel, whereas in the latter case it is perpendicular to the layer planes.

Dielectric measurements were done in a shielded plate condenser described previously.⁷ The distance between the plates was kept between 12 and 70 μm depending on the configuration. The cells were first calibrated using air and toluene as standard references. This calibration allows us to calculate absolute values of the electric permittivity. The samples were put slightly above the cholesteric-isotropic transition point and the measurement cells were filled in by the capillary effect. Orientation of the samples was achieved by putting the cell into a magnetic field of 1.2 T and then it was slowly cooled from the isotropic to the Sm- C^* phase (a few degrees below the transition temperature) with a cooling rate of 3°C per hour. Further thermal processing of the Sm- C^* phase was carried out without a magnetic field. For the perpendicular configuration the orienting magnetic field was

parallel to the glass plates, and in this geometry the ϵ_{\perp} electric permittivity component was measured (Fig. 1). For the parallel configuration the magnetic field was perpendicular to the electrodes (Fig. 1) to measure the ϵ_{\parallel} component. There was no magnetic field while taking the measurements in the smectic phases. The quality of alignment was checked by polarizing microscopy and by watching the time development of the dielectric anisotropy.

The homogeneous alignment was also checked by a surface treatment (rubbing) method^{8,9} as well as by a magnetic field using indium tin oxide (ITO)-coated transparent electrodes. The alignment in both cases was almost the same. The gold-coated electrodes were used because of their low resistivity (one order of magnitude lower) as compared with ITO electrodes. This was important in investigations of the soft mode which shows up in the higher-frequency range.

The frequency and temperature dependences of the real and imaginary part of the electric permittivity have been studied in the frequency range from 5 Hz to 13 MHz. Two different measuring setups were used for the low- and high-frequency regions. For low frequencies in the range between 5 and 500 Hz we used the General-Radio bridge 1641 A with oscillator 1310 and detector 1232 A based upon the transformer ratio arm principle. For higher frequencies up to 13 MHz, the self-balancing Hewlett-Packard bridge 4192 A was used under computer control. The data were corrected for the static conductivity and for the high-frequency deviations caused by the inductance and resistance of the cables and connectors as well.

III. THEORETICAL BACKGROUND

In normal tilted phases (Sm-C, Sm-I, Sm-F, Sm-J, and Sm-G) the local symmetry of rodlike molecules has the

following symmetry elements: a twofold axis (2) of rotation, a mirror plane (m), and a center of inversion ($\bar{1}$). So, the point group is $2/m$. If chiral molecules are added to such systems, the local point symmetry is reduced to the twofold axis of rotation only. This axis is perpendicular to the long molecular axis L . Once the molecule possesses a dipole moment being strongly coupled to a chiral center and perpendicular to the L axis, a spontaneous polarization (P_{\perp}) shows up perpendicular to the (z, L) plane, i.e., parallel to the twofold axis (Fig. 2). To describe ordering of molecules in tilted structures the following order parameter has been introduced:^{5,10}

$$\xi = \hat{x}\xi_1 + \hat{y}\xi_2 = \theta_0(\hat{x} \cos\varphi + \hat{y} \sin\varphi), \quad (1)$$

where \hat{x} and \hat{y} are the respective unit vectors, θ_0 is the tilt angle, and φ is the azimuthal angle. In chiral polar systems the spontaneous polarization P_{\perp} can also be treated as an order parameter,

$$P_{\perp} = \hat{x}P_x + \hat{y}P_y = P[\hat{x}(-\sin\varphi) + \hat{y}\cos\varphi]. \quad (2)$$

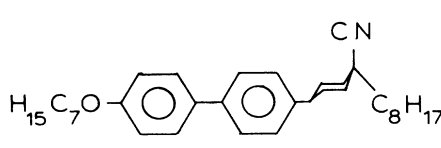
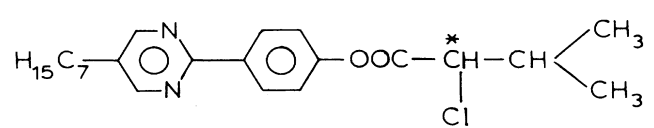
Due to the chirality of molecules there is a systematic change of the φ angle along the z axis on going from one layer to another. This leads to a spectacular helicoidal structure in which both order parameters are spatially modulated,

$$\xi(z) = \theta_0[\hat{x} \cos(qz) + \hat{y} \sin(qz)], \quad (3)$$

$$P_{\perp}(z) = P_0[-\hat{x} \sin(qz) + \hat{y} \cos(qz)], \quad (4)$$

where $q = 2\pi/L_0$ is the wave vector of the helicoidal structure and L_0 is in turn the pitch of the helix. It means that the net polarization of a macroscopic Sm-C* sample is equal to zero. However, due to the linear coupling between the polarization P_{\perp} and external electric field E the helicoidal ordering of the former can be disturbed, leading to an effective polarization along the field,

TABLE I. Two basic compounds of the ZLI-3654 mixture and the phase diagram of the mixture. The standard notations are used in the phase diagram.

No.	Structure of molecule							
(1)								
(2)								
Phase diagram of the ZLI-3654 mixture								
Cr	< -30°C	Sm-C*	62°C	Sm-A*	76°C	N*	86°C	I*

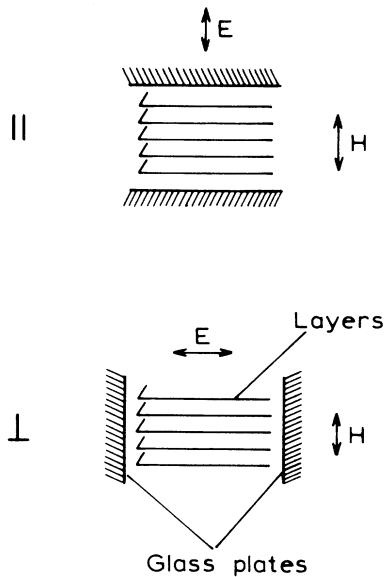


FIG. 1. Configuration for \parallel and \perp alignment in liquid-crystalline ferroelectrics. Here E is the measuring electric field and H is the orienting magnetic field.

$$\mathbf{P}_\perp = \epsilon_0(\epsilon_\perp - 1)\mathbf{E}_\perp, \quad (5)$$

where \mathbf{E}_\perp is the electric field component perpendicular to the helix, ϵ_\perp is the electric permittivity tensor component perpendicular to the helix [actually, $\epsilon_\perp = \frac{1}{2}(\epsilon_{xx} + \epsilon_{yy})$], and ϵ_0 is the electric permittivity of the free space.

In the Sm- C^* phase the ϵ_\perp component of the electric permittivity tensor exhibits, in addition to normal molecular relaxation, a spectacular relaxation region, the so-called Goldstone mode,¹¹ showing up in most cases in the frequency range between a few Hz and about 100 kHz.^{2,5,10,12-20} Additionally, in the vicinity of the Sm- C^* -Sm- A^* transition a second relaxation region appears, the so-called soft mode.^{2,21} The Goldstone-mode

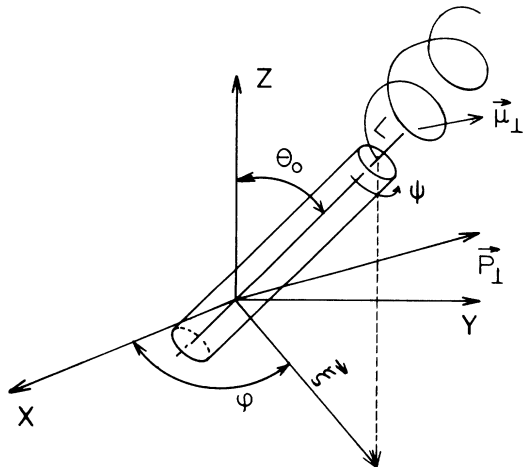


FIG. 2. Local order and symmetry in the Sm- C^* phase.

contribution to the ϵ_\perp electric permittivity is due to fluctuations in phase (φ) of the order parameter, whereas the soft mode comes from the fluctuations of the magnitude of polarization P_0 , i.e., from fluctuations of the tilt angle θ_0 . So, the frequency dependence of the ϵ_\perp component in the Sm- C^* phase can be written as follows:

$$\begin{aligned} \epsilon_\perp^*(\omega) = & \epsilon_{\perp\infty} + \frac{\epsilon_{10}^M - \epsilon_{1\infty}^M}{1 + i\omega\tau_M} + \frac{\epsilon_{10}^G - \epsilon_{1\infty}^G}{1 + (i\omega\tau_G)^{1-\alpha_G}} \\ & + \frac{\epsilon_{10}^S - \epsilon_{1\infty}^S}{1 + (i\omega\tau_S)^{1-\alpha_S}}, \end{aligned} \quad (6a)$$

where $\epsilon_{\perp\infty}$ is the high-frequency limit of the electric permittivity, and $\Delta\epsilon_\perp^M$ (the second term on the right-hand side), $\Delta\epsilon_\perp^G$ (the third term), and $\Delta\epsilon_\perp^S$ (the fourth term) are the dielectric increments coming from the molecular reorientation around the long axis, from the Goldstone mode and from the soft mode, respectively. τ_M , τ_G , and τ_S are the respective relaxation times, and α_G and α_S are the empirical parameters responsible for distribution of the relaxation times. One should explain that in the Sm- A^* phase the contribution coming from the Goldstone mode ($\Delta\epsilon_\perp^G$) is not present and the soft-mode contribution ($\Delta\epsilon_\perp^S$) shows up only few degrees above the Sm- C^* -Sm- A^* transition temperature. On the other hand, in the Sm- C phase in the vicinity of the transition point only the soft mode is present and it is strongly suppressed in the lower-temperature range.^{5,11} However, according to another theoretical prediction the soft mode goes continuously into pure polarization modes far from T_c^z .

In the case of the ϵ_\parallel component only the low-frequency molecular relaxation shows up in both smectic phases. So, the frequency dependence of this component is of the form

$$\epsilon_\parallel^*(\omega) = \epsilon_{\parallel\infty} + \frac{\epsilon_{\parallel 0} - \epsilon_{\parallel\infty}}{1 + (i\omega\tau_\parallel)^{1-\alpha_\parallel}}. \quad (6b)$$

The dielectric increment ($\epsilon_{\parallel 0} - \epsilon_{\parallel\infty}$) is in this case connected with the reorientation of molecules about their short axes. τ_\parallel and α_\parallel are, respectively, the relaxation time and the distribution parameter. Yet in the case of the ϵ_\parallel component there might be some contribution coming from the molecular reorientation around the long axis but in our case it is included in the $\epsilon_{\perp\infty}$ value. Usually, in the case of the low-frequency molecular relaxation one does not observe any distribution of the relaxation times for one-component systems. However, it has been proven experimentally that in the case of mixtures the low-frequency molecular relaxation shows a distribution of the relaxation times.²²

It is worth mentioning that in spite of the Goldstone and soft mode the theory²¹ predicts two additional collective relaxation processes, but up to now they have not been found experimentally as their dielectric increments are very small.

One of the theories of electric permittivities worked out for ferroelectric liquid crystals²¹ predicts the following temperature dependences of the dielectric increments, coming from the Goldstone and soft mode, close to the

transition temperature:

$$\begin{aligned} \Delta\epsilon_1(T < T_c) &= \Delta\epsilon_1^G + \Delta\epsilon_1^S \\ &= \left[\frac{\frac{1}{2}\epsilon_{1\infty} C^2}{\tilde{K}_{33} q^2 C} \right]_G \\ &\quad + \left[\frac{\frac{1}{2}\epsilon_{1\infty}^2 C^2}{2\alpha(T_c - T) + \tilde{K}_{33} q^2 C} \right]_S, \end{aligned} \quad (7a)$$

$$\Delta\epsilon_1(T > T_c) = \Delta\epsilon_1^S = \frac{\epsilon_{1\infty}^2 C^2}{\alpha(T - T_c) + \tilde{K}_{33} q^2 C}, \quad (7b)$$

where C is the piezoelectric bilinear coupling coefficient in the Landau expansion of the free-energy density, \tilde{K}_{33} is the elastic modulus, q is the wave vector of the modulated Sm-C* phase, and α is the temperature coefficient of the quadratic term in the Landau expansion of the order parameter [Eq. (1)] and its derivatives describing different deformations of the helicoidal structure.

IV. RESULTS AND DISCUSSION

In this paper the dielectric relaxation processes are discussed for the Sm-C* and Sm-A* phases of the room-temperature ferroelectric liquid-crystal mixture which exhibits very high spontaneous polarization in the Sm-C* phase. To this end the complex electric permittivity has been measured in wide temperature and frequency ranges. In Sec. IV D the results of our dielectric measurements are reported and discussed in terms of the existing theories.

A. Dielectric anisotropy

In Fig. 3(a) the frequency dependences of the ϵ_{\parallel} and ϵ_{\perp} electric permittivity tensor components as well as the dielectric anisotropy ($\Delta\epsilon = \epsilon_{\parallel} - \epsilon_{\perp}$) measured for the Sm-C* phase at $t = 36^\circ\text{C}$ in the frequency range between 1 kHz and 1 MHz are presented. As is seen the ϵ_{\parallel} component exhibits a low-frequency dispersion region with critical frequency at about 70 kHz, which is in good agreement with the preliminary dielectric measurements done for this mixture.²⁶ This dispersion region is connected with the well-known molecular reorientation about the short molecular axis (see Sec. IV D 3) observed in many polar nonchiral liquid-crystalline systems.^{22,23} On the other hand, the ϵ_{\perp} component is frequency independent in the range from 50 kHz to 1 MHz, which is due to the fact that this component is influenced by the reorientation about the long axes of polar molecules. The contribution to ϵ_{\perp} coming from the last process is pronounced, as one of the substances [(1) in Table I] has a strong dipole moment perpendicular to the long axis. It is also a reason why the dielectric anisotropy is negative in the Sm-C* phase at frequencies above 10 kHz, where the Goldstone-mode contribution is negligible. At frequencies below about 10 kHz there is a critical increase of the ϵ_{\perp} component with decreasing frequency coming from the Goldstone-mode contribution. Frequency dependences of the ϵ_{\parallel} and ϵ_{\perp} components are reflected in the dielectric anisotropy, which is constant ($\Delta\epsilon \approx -2$) in

the high-frequency range (1 MHz) and then increases to about -1.6 due to the low-frequency molecular relaxation, and then eventually decreases critically (below 10 kHz) because of the Goldstone-mode contribution.

The temperature dependence of the dielectric anisotropy acquired at 6.51 kHz is seen in Fig. 3(b). As one can see, $\Delta\epsilon$ is negative in the N*, Sm-A*, and Sm-C* phases, which is caused by the molecular structure of the mixture components having pronounced transverse permanent dipole moment components.²⁶ In the Sm-A* phase close to the transition point, and particularly in the Sm-C* phase, the ϵ_{\perp} component is enhanced by the spontaneous polarization.

B. Thickness dependence of the ϵ_1 component

The dielectric measurements of the ϵ_{\perp} component for the Sm-C* phase seem to be strongly sensitive to the boundary conditions. In Fig. 4 one can see the thickness dependence of ϵ_{\perp} measured in the frequency range from about 100 Hz to 100 kHz. The differences in the ϵ_{\perp} values become important at frequencies below 10 kHz, where the Goldstone-mode contribution dominates the dielectric behavior. In this study most of the dielectric measurements for homogeneous orientation have been

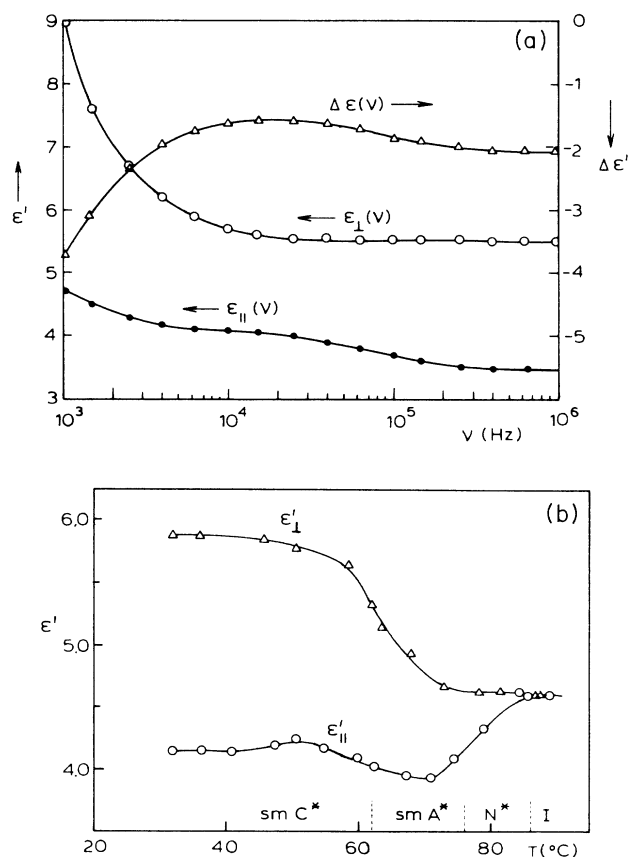


FIG. 3. (a) Frequency dependence of the ϵ'_{\perp} and ϵ'_{\parallel} components and dielectric anisotropy $\Delta\epsilon$ at 36°C temperature. (b) Temperature dependences of two principal electric permittivities, ϵ'_{\perp} and ϵ'_{\parallel} at 6.51-kHz frequency.

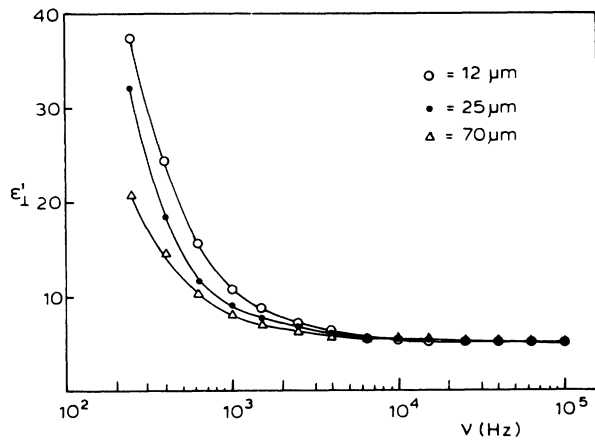


FIG. 4. Thickness dependence of the Goldstone-mode contribution at 36°C temperature.

performed on the 12- μm -thick sample. However, to get the homeotropic texture for measurements on the ϵ_{\parallel} component one should take advantage of thicker samples (25 or 70 μm) aligned by means of the magnetic field.

C. Temperature dependences of the ϵ_1^* component at different frequencies

To study the dielectric relaxation process showing up in the Sm-C* phase due to the Goldstone mode, precise measurements of the complex dielectric permittivity ($\epsilon_1^* = \epsilon_1' - i\epsilon_1''$) have been made in the frequency range between 5 Hz and about 10 kHz. In Fig. 5(a) the temperature dependences of ϵ_1' obtained at different frequencies are presented for the I*, N*, Sm-A*, and Sm-C* phases. As is seen there is practically no dispersion effect in the I*, N*, and Sm-A* phases in the frequency range studied. In this frequency and temperature range a static dielectric constant ϵ_{10} of about 5.0 has practically been observed. However, in the vicinity of the transition temperature Sm-A*–Sm-C* phase a dispersion effect starts, and then below the T_{c2} ferroelectric transition temperature (see Sec. IV D 2) there is a tremendous dispersion effect connected with the Goldstone mode. It is worth pointing out that at these frequencies (5010, 1010, 660, 410, 260, 170, 95, 65, 36, 21, 9, and 5 Hz) characteristic broad maxima, found also for other liquid-crystalline ferroelectrics,^{12,13,15} are present. The dielectric measurements below 5 Hz were cumbersome because of the conductivity contribution.

The frequency dependences of the real part ϵ_1' of the complex electric permittivity is shown in Fig. 5(b). As is seen, the electric permittivities measured at low frequencies are very high and strongly temperature dependent, and above the T_{c2} ferroelectric transition temperature there is practically no contribution originating from the spontaneous polarization. One should stress that the dispersion curves obtained in this study are qualitatively very much similar to those obtained for other ferroelectric materials^{12–20} except for the fact that our material shows very high electric permittivity and the measure-

ments have for the first time been extended to the lowest frequency limit possible for such materials. It is seen in Fig. 5(c) that the measurements could not have been extended to the sub-hertz region due to the pronounced conductivity contribution which is also strongly temperature dependent.

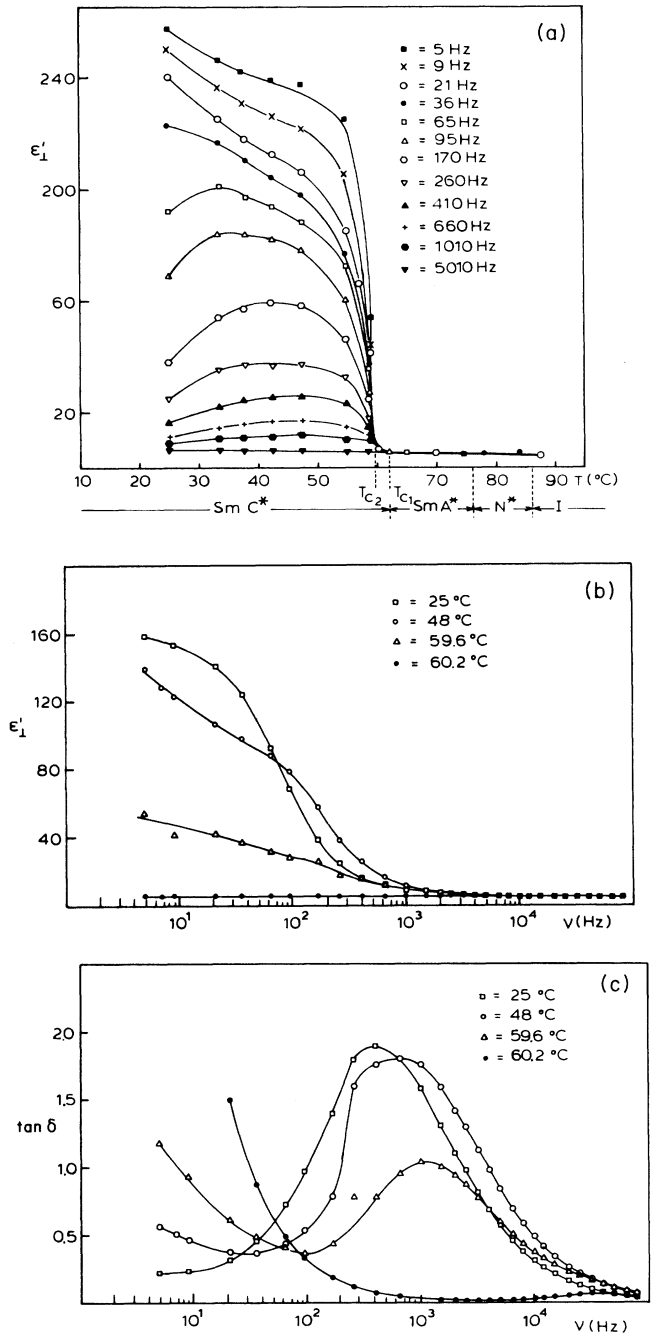


FIG. 5. (a) ϵ_1' component measured as a function of temperature at different frequencies between 5 Hz and 5.01 kHz. (b) Dispersion curves ϵ_1' vs ν obtained for the Sm-C* phase at different temperatures. (c) Frequency dependences of $\tan \delta$ (loss factor) ($\tan \delta = \epsilon'' / \epsilon'$) measured at different temperatures in the Sm-C* phase.

D. Dielectric relaxation processes in the Sm-C* and Sm-A* phases

Up to now we have been discussing qualitatively temperature and frequency dependences of two principal components of the electric permittivity, ϵ_{\perp}^* and ϵ_{\parallel}^* , to show all dielectric anomalies attributed to the liquid-crystalline ferroelectric state studied. In Secs. IV D 1 and IV D 2 a quantitative analysis of the dielectric relaxation processes is presented in terms of the Goldstone and soft modes introduced in Ref. 21.

1. Goldstone mode in the Sm-C* phase

By using a wide-band dielectric spectrometer the dielectric spectra in the Sm-C* phase of the ZLI-3654 mixture have been measured in a broad frequency range from 5 Hz to 13 MHz. Close to room temperature (at $t=25^{\circ}\text{C}$) the dielectric spectrum connected with the Goldstone mode shows up between 10 kHz and 5 Hz. This dielectric spectrum is presented in the form of the dispersion and absorption curves [Fig. 6(a)] as well as the Cole-Cole diagram [Fig. 6(b)]. By fitting to the experimental points the Cole-Cole modification of the Debye equation,

$$\epsilon_{\perp}^* = \epsilon_{\perp\infty} + \frac{\epsilon_{10}^G - \epsilon_{\perp\infty}^G}{1 + (\omega\tau_G)^{1-\alpha_G}}, \quad (8)$$

the following dielectric parameters have been computed: ϵ_{10}^G , the static dielectric constant for the Goldstone mode; $\epsilon_{\perp\infty}^G$, the high-frequency limit of the electric permittivity for the Goldstone mode; it is a sum of two contributions, $\epsilon_{1\infty}^G = 1.05n_1^2 + \Delta\epsilon_M$ (n_1 is refractive index); τ_G , the dielectric relaxation time for the Goldstone mode being a good measure of the switching time of electro-optic cells; and α_G , the distribution parameter. Table II contains the dielectric parameters obtained for the Goldstone mode at different temperatures in the Sm-C* phase. In Fig. 7 the dielectric spectrum, obtained in the vicinity of the ferroelectric transition temperature T_{c2} , is shown. This spectrum might be influenced by both the Goldstone and the soft mode which is obvious from the theoretical standpoint.^{2,21} However, any splitting of this spectrum into two relaxation regions is, at the moment, fully unsubstantiated. Yet we are inclined to treat the soft mode as an extreme case of the Goldstone mode due to the continuous changes of the dielectric increments in the vicinity of the transition point which is also predicted by

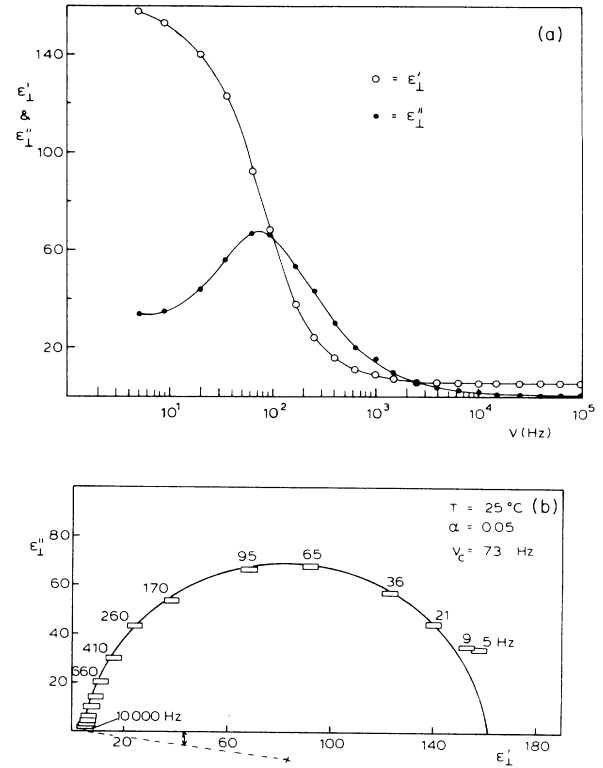


FIG. 6. (a) Dispersion and absorption curves obtained for the Goldstone mode at 25°C . (b) Cole-Cole representation of the Goldstone mode at 25°C temperature.

another theory.³ In Sec. IV D 2 it will be shown that the spectrum taken at 60°C is more soft-mode-like.

2. Soft mode in the vicinity of the transition temperature

As we have seen in Figs. 5(a)–5(c) and also in Figs. 6(a) and 6(b), in the Sm-C* phase there is a pronounced dispersion region below 1 kHz connected with the Goldstone mode. However, if one magnifies the ϵ'_{\perp} scale [Fig. 8(a)] above the T_{c2} transition temperature a new relaxation region shows up, but its dispersion takes place at much higher frequencies (between 1 kHz and 1 MHz) in comparison to the Goldstone mode. In addition, the dielectric increment for this pretransition relaxation region is critically temperature dependent and vanishes a

TABLE II. Dielectric parameters of the Goldstone mode.

t ($^{\circ}\text{C}$)	ν_c^G (Hz)	τ_G (ms)	ϵ_{10}^G	$\epsilon_{\perp\infty}^G$	α_G
25	73.0	2.179	161.38	5.440	0.085
33.4	119.8	1.329	157.77	5.198	0.099
37.8	118.9	1.339	158.17	5.128	0.105
42.6	117.5	1.355	159.61	5.056	0.108
47.4	114.5	1.390	165.77	4.990	0.112
55.2	80.0	1.989	328.39	4.850	0.139
59.6	353.3	4.500	43.396	5.311	0.094
60.0	6463.0	0.025	8.538	4.940	0.114

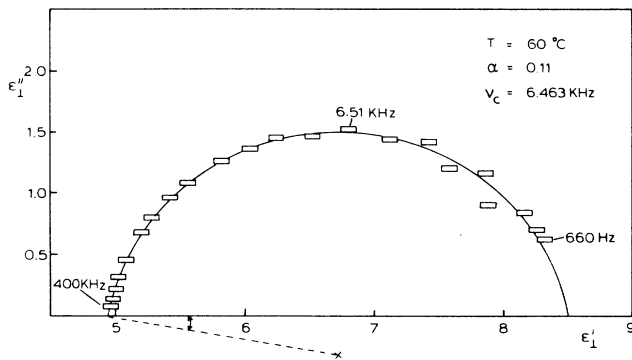


FIG. 7. Cole-Cole diagram for the Goldstone mode in the vicinity of the transition temperature T_{c2} .

few degrees above the T_{c1} temperature, which is a $Sm-C^*$ transition recorded by the texture observations. It is known that texture observations always give the highest temperature. In our case one might also think a biphasic region observed for other mixtures. As will be shown below one can conclude from our dielectric data that the ferroelectric first-order phase transition is at the T_{c2} temperature, where a movement of the disclination lines has also been seen. Such an effect has also been observed by other authors.¹⁵ In Figs. 8(b) and 8(c) the soft mode is presented in form of the Cole-Cole plots. By fitting the Cole-Cole formula to the experimental data the dielectric parameters for the soft mode have been calculated. They are gathered in Table III. It is worth stressing that the dielectric increment ($\Delta\epsilon^S = \epsilon_{10}^S - \epsilon_{1\infty}^S$) of the soft mode obeys the Curie-Weiss law (Fig. 9) with the critical temperature T_{c2} . The fit to the experimental data gives us the ferroelectric transition temperature, $T_{c2} = 59.82^\circ C$.

As one can see from Table II, temperature dependence of the Goldstone-mode critical frequency is very weak, and in the range from 37.8 to $55.2^\circ C$ it is almost constant. Such a non-Arrhenius-type behavior of the Goldstone mode is also predicted by the theory. On the other hand, the soft-mode critical frequencies as well as the relaxation times behave critically in the vicinity of the transition point. The slope of the Arrhenius plot below T_{c1} , amounting to $E = 805$ kJ/mole (8.2 eV/particle), is twice the respective value found above T_{c1} $E = 395$ kJ/mole (4.03 eV/particle). These very high values of the activation energies suggest that the soft mode is a collective molecular process resembling the α -relaxation process observed for polymers above the glassy transition.²⁴

3. Low-frequency molecular relaxation in the $Sm-C^*$ and $Sm-A^*$ phases

As was mentioned above, in polar liquid crystals two principal molecular reorientations, i.e., the reorientation around the short and long molecular axes, give separate dielectric relaxation regions falling within the radio and microwave frequency ranges.^{22,23} From our experimental data it is clearly seen that both molecular motions give contributions to the electric permittivities. The fact that the $\epsilon_{1\infty}$ values for the Goldstone mode (Table II) as well

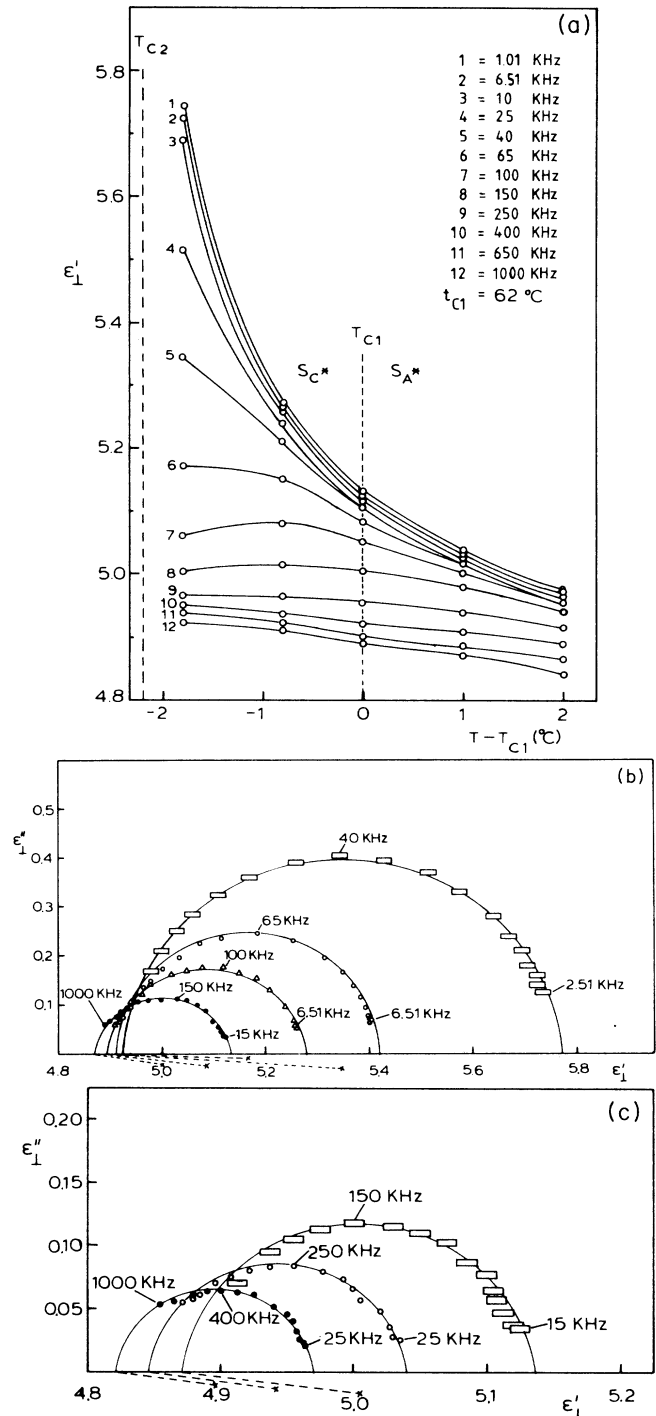


FIG. 8. (a) Temperature dependences of the electric permittivities measured at different frequencies in the vicinity of the $Sm-C^*$ - $Sm-A^*$ transition temperature. (b) Cole-Cole representation of the dielectric spectrum of the soft mode below the T_{c1} temperature, for $t = 60.2^\circ C$ (\circ), $\alpha = 0.04$, and $\nu_c = 37.64$ kHz; for $t = 60.8^\circ C$ (\circ), $\alpha = 0.03$, and $\nu_c = 72.85$ kHz; for $t = 61.2^\circ C$ (Δ), $\alpha = 0.07$, and $\nu_c = 87.99$ kHz; and for $t = 62.0^\circ C$ (\bullet), $\alpha = 0.10$, and $\nu_c = 162.79$ kHz. (c) Cole-Cole plots for the soft-mode dielectric spectrum above the T_{c1} temperature; for $t = 62.1^\circ C$ (\circ), $\alpha = 0.01$, and $\nu_c = 162.70$ kHz; for $t = 63.0^\circ C$ (\circ), $\alpha = 0.08$, and $\nu_c = 248.08$ kHz; and for $t = 64.0^\circ C$ (\bullet), $\alpha = 0.08$, and $\nu_c = 377.48$ kHz.

TABLE III. Dielectric relaxation parameters of the soft mode.

Phase	t ($^{\circ}\text{C}$)	ν_c^S (kHz)	τ_S (μs)	ϵ_{10}^S	$\epsilon_{1\infty}^S$	α_S
Sm-C*	60.0	6.463	24.63	8.538	4.940	0.115
	60.2	37.670	4.23	5.769	4.926	0.043
	60.8	72.850	2.19	5.417	4.917	0.027
	61.2	87.994	1.81	5.280	4.894	0.069
Sm-A*	62.1	162.704	0.978	5.137	4.869	0.101
	63.0	248.090	0.641	5.040	4.849	0.080
	64.0	377.480	0.422	4.971	4.825	0.075

as for the soft mode (Table III) are distinctly higher than the n_1^2 , shows that in the high-frequency range (1 GHz) there must be an additional dispersion process connected with the reorientation of molecules around their long axes.

Additional dispersion measurements done by us for the ϵ_{\parallel}^* component revealed the existence of the low-frequency molecular relaxation in both smectic phases. The dielectric spectra obtained are presented in Figs. 10(a) and 10(b), respectively. By fitting Eq. (6b) to the experimental points the dielectric parameters gathered in Table IV have been calculated. As is seen the critical frequencies

of the molecular relaxation are much higher than those obtained from the Goldstone and the soft modes. It is worth pointing out that the molecular relaxation exhibits a distribution of the relaxation times which is consistent with the results obtained for other liquid-crystalline mixtures.²² The activation energies calculated for the low-frequency molecular relaxation are in both phases of

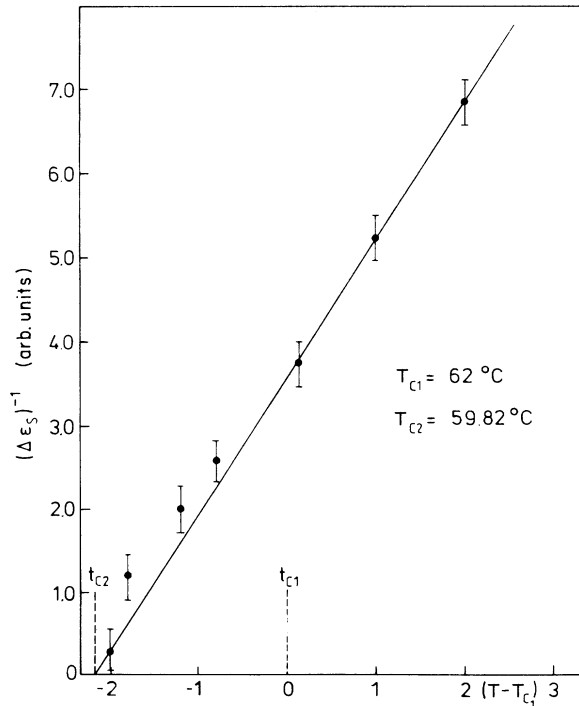


FIG. 9. Curie-Weiss plot for the dielectric increment of the soft mode.

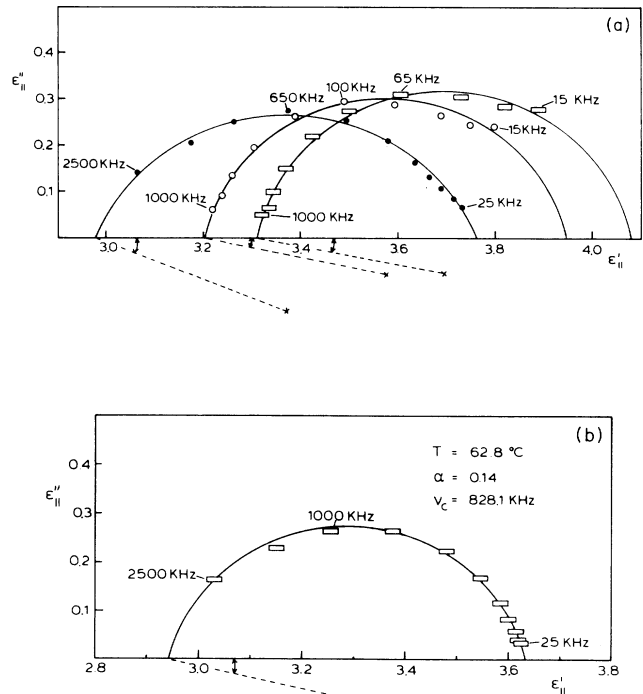


FIG. 10. Cole-Cole representation of the low-frequency molecular dielectric spectrum taken at different temperatures in the Sm-C* phase, for $t = 32.0^{\circ}\text{C}$ (\square), $\alpha = 0.12$, and $\nu_c = 40.74$ kHz; for $t = 37.0^{\circ}\text{C}$ (\circ), $\alpha = 0.13$, and $\nu_c = 59.18$ kHz; and for $t = 60.0^{\circ}\text{C}$ (\bullet), $\alpha = 0.24$, and $\nu_c = 592.73$ kHz. (b) Molecular low-frequency dielectric spectrum in the Sm-A* phase.

about 100 kJ/mole which is the typical value found for the smectic- C and smectic- A phases.^{22,23}

E. Critical frequencies for different relaxation modes

A comparison of the critical frequencies obtained by us for the low-frequency molecular relaxation and for the Goldstone and soft modes is presented in Fig. 11. As is seen the soft mode is only present above the T_{c2} transition point. The fact that the ferroelectric transition temperature is below the T_{c1} transition temperature, found by texture observations, suggests that the transition between the $Sm-C^*$ and $Sm-A^*$ phase might be of the first-order type as it was found for other liquid-crystalline mixtures with very high spontaneous polarization.²⁰

V. CONCLUSIONS

(a) In the $Sm-C^*$ phase of the ZLI-3654 mixture a very high contribution to the electric permittivity was found and assigned to the Goldstone mode. It is a collective process showing a non-Arrhenius-type behavior of the critical frequencies.

(b) In the vicinity of the $Sm-C^*-Sm-A^*$ transition point the Goldstone-mode contribution to the electric permittivity drastically decreases. Above the ferroelectric transition temperature only the soft mode contributes to the ϵ_{\perp} component, and its dielectric increment fulfills the Curie-Weiss law with the T_{c2} critical temperature. From the dielectric data presented in this study one can conclude that the phase transition between the $Sm-C^*$ and $Sm-A^*$ phases is most probably of the first-order type. Further studies of this transition by using calorimetric methods should be undertaken. However, our preliminary differential scanning calorimetry (DSC)

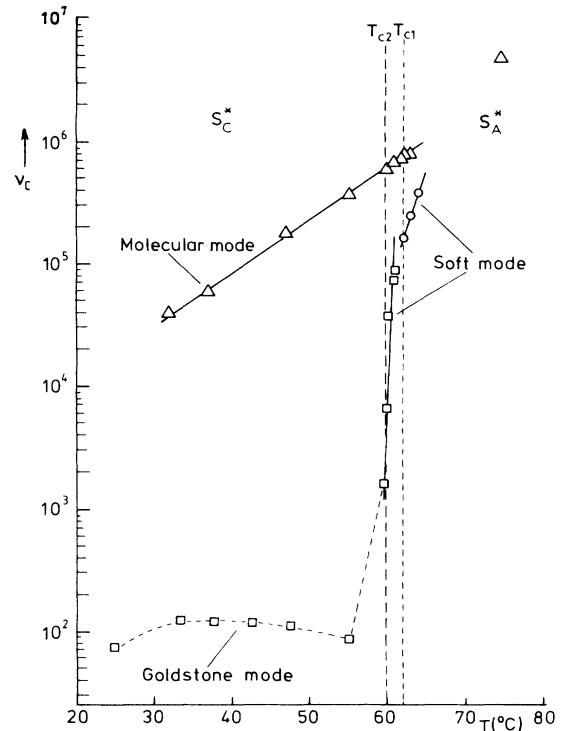


FIG. 11. Critical frequencies vs temperature obtained for different relaxation modes in the $Sm-C^*$ and $Sm-A^*$ phases.

observations do not give a unique answer.

(c) In both smectic phases the low-frequency molecular relaxation was also found for the ϵ_{\parallel} component, and its critical frequencies are distinctly higher than the respective values found for the soft mode even in the neighborhood of the phase transition.

TABLE IV. Low-frequency molecular relaxation.

Phase	t (°C)	ν_{\parallel} (kHz)	τ_{\parallel} (μ s)	$\epsilon_{\parallel 0}$	$\epsilon_{\parallel \infty}$	α_{\parallel}
$Sm-C^*$	32	40.74	3.907	4.086	3.309	0.124
	37	59.18	2.689	3.947	3.203	0.134
	47	117.21	0.898	3.754	3.049	0.150
	55.2	362.10	0.439	3.773	3.014	0.241
	60.0	592.73	0.269	3.758	2.977	0.237
	61.0	683.80	0.233	3.716	2.984	0.183
$Sm-A^*$	62.0	757.88	0.210	3.672	2.965	0.158
	62.4	757.77	0.199	3.667	2.965	0.148
	62.8	828.07	0.192	3.637	2.945	0.143
	74.8	3095.07	0.0514	3.681	2.994	0.079

ACKNOWLEDGMENTS

The authors sincerely thank E. Merck Co. for supplying us with the material ZLI-3654. Fruitful discussions with Dr. T. Geelhaar (E. Merck) and Dr. F.-J. Bormuth

(Technische Hochschule) are gratefully acknowledged. A.M.B. thanks the Deutscher Akademischer Austauschdienst e.V. for financial assistance. S.W. is thankful to the Technical University of Darmstadt for financial support during his stay.

-
- *Permanent address: National Physical Laboratory, Dr. K. S. Krishnan Road, New Delhi-110012, India.
- †Permanent address: Institute of Physics, Jagellonian University, 30059 Krakow, Reymonta 4, Poland.
- ¹R. B. Meyer, L. Liebert, L. Strzelecki, and P. Keller, *J. Phys. Lett. (Paris)* **36**, L69 (1975).
- ²B. Žekš, A. Levstik, and R. Blinc, *J. Phys. (Paris) Colloq.* **40**, C3-409 (1979).
- ³Ph. Martinot-Lagarde and G. Durand, *J. Phys. (Paris)* **42**, 269 (1981).
- ⁴L. G. Benguigui, *J. Phys. (Paris)* **43**, 915 (1982).
- ⁵A. Levstik, T. Carlsson, C. Filipič, I. Levstik, and B. Žekš, *Phys. Rev. A* **35**, 3527 (1987).
- ⁶T. Geelhaar (private communication from E. Merck Co., Darmstadt).
- ⁷W. Haase, H. Pranoto, and F.-J. Bormuth, *Ber. Bunsenges. Phys. Chem.* **89**, 1229 (1985).
- ⁸J. S. Patel, T.M. Leslie, and J. W. Goodby, *Ferroelectrics* **59**, 137 (1984).
- ⁹S. S. Bawa, A. M. Biradar, and S. Chandra, *Ferroelectrics* **76**, 69 (1987).
- ¹⁰P. G. de Gennes, *Physics of Liquid Crystals* (Clarendon, Oxford, 1974).
- ¹¹A. Levstik, T. Carlsson, C. Filipič, and B. Žekš, *Mol. Cryst. Liq. Cryst.* **154**, 259 (1988).
- ¹²B. I. Ostrovski, A. Z. Rabinovich, A. S. Sonin, and B. A. Strukov, *Zh. Eksp. Teor. Fiz.* **74**, 1448 (1978).
- ¹³J. Hoffmann, W. Kuczynski, and J. Malecki, *Mol. Cryst. Liq. Cryst.* **44**, 287 (1978).
- ¹⁴I. Musšvič, B. Žekš, R. Blinc, Th. Rasing, and P. Wyder, *Phys. Status Solidi B* **119**, 727 (1983).
- ¹⁵M. Glogarova, J. Pavel, and J. Fousek, *Ferroelectrics* **55**, 117 (1984).
- ¹⁶L. G. Benguigui, *Ferroelectrics* **58**, 269 (1984).
- ¹⁷K. Yoshino, M. Ozaki, H. Agawa, and Y. Shigeno, *Ferroelectrics* **58**, 283 (1984).
- ¹⁸R. J. Cava, J. S. Patel, K. R. Collen, J. W. Goodby, and E. A. Rietman, *Phys. Rev. A* **35**, 4378 (1987).
- ¹⁹L. Bata, A. Buka, N. Éber, A. Jáklí, K. Pintér, J. Szabon, and A. Vajda, *Mol. Cryst. Liq. Cryst.* **151**, 47 (1987).
- ²⁰Ch. Bahr, G. Heppke, and N. K. Sharma, *Ferroelectrics* **76**, 151 (1987).
- ²¹R. Blinc and B. Žekš, *Phys. Rev. A* **18**, 740 (1978).
- ²²H. Kresse, *Advances in Liquid Crystals*, edited by G. H. Brown (Academic, New York, 1983), Vol. 6, p. 109.
- ²³J. P. Parneix, C. Legrand, and D. Decoster, *Mol. Cryst. Liq. Cryst.* **98**, 361 (1983); S. Wróbel, *ibid.* **127**, 67 (1985).
- ²⁴H. Pranoto, F.-J. Bormuth, and W. Haase, *Makromol. Chem.* **187**, 2453 (1986); F.-J. Bormuth, Ph.D. thesis, Darmstadt, 1988 (unpublished).